

Dimensional cross-over and charge order in half-doped Manganites and Cobaltites

Oron Zachar^{1,2} and Igor Zaliznyak¹

¹Brookhaven National Laboratory, Upton, New York 11973-5000 USA. and

²UCLA Dep. of Physics, Los Angeles, CA 90095, USA.

We introduce a general model for understanding the effect of quenched disorder on charge ordering in half-doped Manganese- and Cobalt-Oxides with different crystal structures. Current experimental results (Table-1) are discussed in light of the global phase diagram of the model (Fig. 2).

In the past decade much theoretical work was devoted to elucidating the nature and origin of charge ordering (CO) in the doped transition metal oxides, particularly in manganites, which are of great experimental and practical interest [1, 2, 3]. At half-doping the low temperature ground state of many Mn oxides and isostructural Co oxides manifests a checkerboard-type planar charge modulation shown in Fig. 1, and concomitant Jahn-Teller (JT) distortion of the MO_6 ($M = \text{Mn, Co, etc.}$) octahedra [4, 5, 6]. In manganites much attention was paid to studying orbital and antiferromagnetic correlations which usually accompany or follow the CO. Yet, the effect of quenched disorder on the charge order (distinguished from orbital order) was thus far ignored. A random distribution of the dopant ions is a source of an unavoidable random potential, which couples linearly to any charge density fluctuation [3]. By taking account of this random potential we arrive at a general model (1) and construct the phase diagram (Fig. 2), describing charge ordering in half-doped transition metal oxides such as manganites and cobaltites.

As a general framework, we argue that hopping dynamics, orbital, magnetic, local Coulomb and Jahn-Teller interactions can all be integrated out into an effective primary charge-ordering interaction which then competes with the random charge potential due to the dopant ions. Since a charge order parameter is associated with ionic valence alone, we may drop any reference to orbital and spin indices. To be explicit, we present the model construction in terms of $\text{La}_{1.5}\text{Sr}_{0.5}\text{CoO}_4$ [5]. It has CO similar to that in half-doped manganites but no superimposed

further symmetry breaking due to orbital order.

At low temperature the electrons are highly localized in a charge-ordered state with alternating Co^{2+} and Co^{3+} ions (Mn^{4+} and Mn^{3+} in manganites). There is a concomitant JT distortion of the oxygen octahedra such that in-plane O^{2-} ions move towards the higher-valence Co^{3+} . This is schematically depicted in Fig. 1, where ab plane is tiled with cells $\{\mathbf{r}\}$ containing two cobalt ions. A perfectly ordered state has a two-fold degeneracy associated with the choice of sublattice occupied by the higher/lower valence ions. We define a local Ising variable $\tau(\mathbf{r}) = \pm 1$, to denote the two alternative ionic configurations. A single-domain CO state corresponds to a ferromagnetic order of $\tau(\mathbf{r})$. Topological disorder is introduced by domain walls as shown in Fig. 1(d). In principle, the model can be enriched by introducing ‘vacancies’, $\tau(\mathbf{r}) = 0$, which represent cells with an even number of electrons, but we shall exclude such possibilities from the model, analysis, and discussion of the present paper.

Because of the Jahn-Teller distortion, there is an elastic strain energy cost for nearest neighbor cells with opposite τ values, Fig. 1(d). This strain energy can be described by an effective short-range ferromagnetic interaction $J(\mathbf{r} - \mathbf{r}')\tau(\mathbf{r})\tau(\mathbf{r}')$ [7]. Without a loss of generality we may approximate $J(\mathbf{r} - \mathbf{r}')$ by nearest-neighbor coupling. The potential introduced by dopant atoms randomly favor one or the other configuration of a two-ion cell, and thus act as an effective random external field $h(\mathbf{r})\tau(\mathbf{r})$. Importantly, due to the crystal structure the effective coupling is anisotropic, $J_c \neq J_{ab}$. Hence, for the charge order, the effect of elastic crystal strain and random dopant distribution is captured by an effective *anisotropic* random-field-Ising-model (RFIM). To our knowledge, all previous analytical and numerical work dealt exclusively with the isotropic 3D RFIM. Here we make the first attempt aimed at a qualitative and quantitative understanding of the anisotropic RFIM,

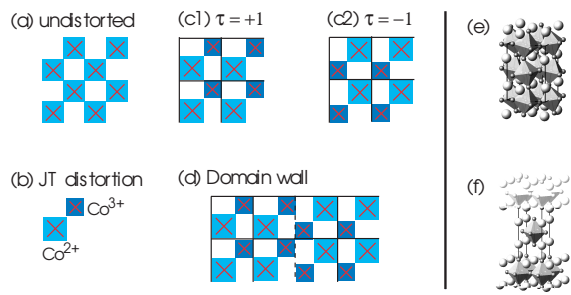


FIG. 1: Charge order and JT distortion in $\text{La}_{1.5}\text{Sr}_{0.5}\text{CoO}_4$.

$$H = -J_{ab} \sum_{\langle \mathbf{r} \mathbf{r}' \rangle_{ab}} \tau_{\mathbf{r}} \tau_{\mathbf{r}'} - J_c \sum_{\langle \mathbf{r} \mathbf{r}' \rangle_c} \tau_{\mathbf{r}} \tau_{\mathbf{r}'} + \sum_{\mathbf{r}} h_{\mathbf{r}} \tau_{\mathbf{r}}, \quad (1)$$

where $\langle \mathbf{r} \mathbf{r}' \rangle_{ab}$ and $\langle \mathbf{r} \mathbf{r}' \rangle_c$ denote nearest-neighbor cells in the ab -plane and along the c -axis, respectively.

Random fields alter both the lower critical dimension [8] and critical exponents [9] of an Ising system. In particular, for weak random fields $\Delta/J \ll 1$ (where J and

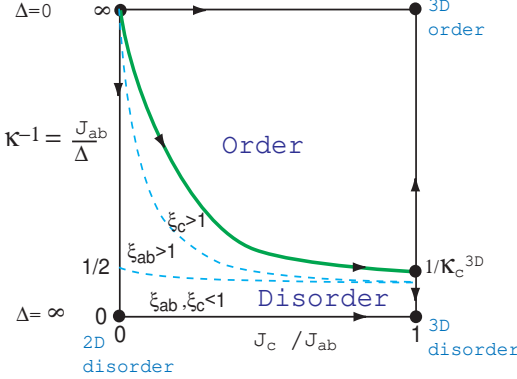


FIG. 2: Charge order phase diagram obtained from the anisotropic random field Ising model. J_c/J_{ab} parametrizes the anisotropy of effective coupling. J_{ab}/Δ parametrizes the relative strength of disorder potential from the dopant ions.

$\Delta = \{\text{rms of } h_r\}$ characterize the Ising coupling and disorder potential respectively) an isotropic 3D RFIM orders at finite temperature $T_c > 0$, while a 2D RFIM has no long range order (LRO) even at $T = 0$. Hence, we pose the question: what is the fate of an anisotropic 3D random field Ising model? The simplest way of connecting the renormalization group (RG) flows leads us to conjecture the phase diagram shown in Fig. 2.

Because the isotropic 3D RFIM is long-range ordered for $\Delta/J < 2.27$ [17], it is clear that when $\Delta < J_c < J_{ab}$ the system is in the regime of weak 3D disorder and has a 3D LRO. Thus, we are lead to examine the a-priory ambiguous case, where bare model parameters satisfy

$$J_c \ll \Delta < J_{ab}, \quad (2)$$

i.e., the c -axis coupling is in the regime of *strong* disorder, while ab -planes are in the weak disorder limit.

To connect our model analysis with experiments, we summarize in Table-I the charge order correlation lengths ξ_{ab} in the ab -plane and ξ_c along the c -axis, measured in several representative compounds. Correlations in the pseudo-cubic systems I-III are resolution-limited (typically this means $\xi \gtrsim 2000 \text{ \AA}$ [11, 12]), and CO is apparently long-range. On the other hand, in the layered sys-

TABLE I: Correlation lengths in terms of number of unit cells in each direction (i.e. ξ_c in units of $c \approx 12.5 \text{ \AA}$, and ξ_{ab} in units of $a\sqrt{2} \approx 5.44 \text{ \AA}$, as implied by Fig. 1).

#	Material	Ref.	ξ_{ab}	ξ_c
I.	$\text{La}_{0.5}\text{Ca}_{0.5}\text{MnO}_3$	[11]	∞	∞
II.	$\text{Pr}_{0.5}\text{Ca}_{0.5}\text{MnO}_3$	[12]	∞	∞
III.	$\text{Nd}_{0.5}\text{Sr}_{0.5}\text{MnO}_3$	[13]	∞	∞
IV.	$\text{La}_{0.5}\text{Sr}_{1.5}\text{MnO}_4$	[4]	≈ 35	≈ 2.5
V.	$\text{La}_{1.5}\text{Sr}_{0.5}\text{CoO}_4$	[5]	≈ 5.5	$\lesssim 1$

tems IV-V the CO is finite-range with highly anisotropic 3D correlations $\xi_{ab} \gg \xi_c$, which implies $J_{ab} \gg J_c$. Large in-plane correlation length $\xi_{ab} \gg 1$ indicates weak planar disorder $\Delta \ll J_{ab}$. Therefore, the materials under consideration probe exactly the most interesting and complicated region of the phase diagram.

For $J_c = 0$ the system decouples into independent 2D RFIM planes, and the ground state is disordered. This form of disordered ground state is perturbatively stable (an underlying assumption of any previously claimed experimental realizations of 2D RFIM systems [3]). i.e., for infinitesimal inter-plane coupling $J_c/\Delta \ll 1$, the ab -planes remain uncorrelated on all length scales (c -axis correlation length $\xi_c < 1$), and each plane may still be treated as an effectively independent 2D RFIM. Therefore, a line of the phase transitions exists in the $(J_{ab}/\Delta, J_c/J_{ab})$ phase diagram, separating the disordered and 3D LRO phases (solid green line in Fig. 2). Increasing J_c/J_{ab} on the disordered side, we enter an interesting critical regime, where the ground state is still disordered, but with significant (albeit highly anisotropic) correlations in all spacial directions. In isotropic 1D, 2D, and 3D RFIM, the ground state correlation length scales with $\kappa = \Delta/J$ as $\xi^{1D} \approx \kappa^{-2}$, $\xi^{2D} \approx \exp(\frac{1}{\sigma}\kappa^{-2})$, and $\xi^{3D} \approx (\kappa - \kappa_c)^{-\nu}$ (for $\kappa \geq \kappa_c \approx 2.27$ [17]), correspondingly [10]. How do the correlation lengths behave in a highly anisotropic 3D RFIM system where $J_c \ll \Delta < J_{ab}$?

The phase diagram instructs us that upon RG transformation model (1) scales either to a 3D LRO fixed point, or towards a 3D strong disorder fixed point. Currently, there is no generally satisfying analytical derivation of RG equations for the RFIM in less than 4D. We introduce a new phenomenological scaling equation for the 2D RFIM, and perturbative RG equations for the anisotropic 3D RFIM with which we attempt to trace out the form of the phase diagram. Moreover, we use our scaling equation to quantitatively estimate the anisotropic correlation lengths as a function of J_c, J_{ab} and Δ , and estimate the cross-over line in the phase diagram.

For isotropic RFIM, the dimensional analysis of Imry-Ma, $\{J(l) = Jl^{d-1}; \Delta(l) = \sqrt{l^d}\Delta\}$, predicts the scaling behavior of $\kappa = \frac{\Delta}{J}$ to be [8, 16]

$$\kappa(l) = \frac{\Delta(l)}{J(l)} \approx \frac{\sqrt{l^d}}{l^{d-1}} \kappa \quad (3)$$

The marginality of $\kappa(l)$ in two dimensions (associated with $d = 2$ being the lower critical dimension) is broken by subdominant contributions from interface roughening at the domain boundaries, and lead to a disordered ground state [10]. For weak disorder, $\kappa \ll 1$, the correlation length $\xi = A \exp\{+\frac{1}{\sigma}\kappa^{-2}\}$ with $A, \sigma \approx 1$. (Clearly this expression for ξ makes no sense for strong disorder where $\xi \leq 1$). Under RG scaling, at the commonly used level of approximation where the generation of additional

longer range interactions is neglected, we phenomenologically require the self consistency of the scaling equations for $\kappa(l)$ and $\xi(l) = \xi/l$ with the correlation length expression, i.e., $\xi(l) = A \exp\left\{+\frac{1}{\sigma}\kappa^{-2}(l)\right\}$. Consequently, we argue that the scaling equation for $\kappa(l)$ in 2D is

$$\kappa^{-2}(l) = \kappa^{-2}\left[1 - \kappa^2\sigma \ln(l)\right] \quad (4)$$

The disordered groundstate is evidenced by the flow of $\kappa^{-1}(l) = \frac{J(l)}{\Delta(l)} \rightarrow 0$.

Turning on weak inter-plane coupling J_c , we shall derive the qualitative features of the RG flows in Fig. 2. That the fixed points all lay on the isotropic line $J_c/J_{ab} = 1$ is evidence to the general idea that the anisotropy of interaction is an irrelevant perturbation at the critical point. At mean-field level (and without random fields) the anisotropy of interactions can be removed by an anisotropic rescaling of coordinates[16]. We shall implement this idea within a real-space block RG procedure by coarse-graining to anisotropic blocks $l_{ab} \times l_{ab} \times l_c$, and demonstrate explicitly the flow towards the isotropic fixed points. We define anisotropy parameter $\alpha = \left(\frac{J_c}{J_{ab}}\right)^{\frac{1}{x}}$, (and $x < 1$), and choose the block size to be $\{l_{ab} = l ; l_c = l^\alpha\}$. i.e., the shape of the coarse graining blocks is itself gradually varying, progressing from anisotropic towards isotropic. The resulting perturbative RG equations are

$$\frac{d(\kappa^2)}{d \ln(l)} = -\alpha\kappa^2 + \sigma\kappa^4 + \mathcal{O}(\alpha^2) \quad (5)$$

$$\frac{d\alpha}{d \ln(l)} = x(1 - \alpha)\alpha \quad (6)$$

We obtain an unstable fixed point at $\alpha^* = 0$ and stable fixed points at $\alpha^* = 1$. The 3D critical fixed point is then at $\kappa_c = \sqrt{\alpha^*/\sigma}$. In principle, numerical integration would allow for the determination of the phase transition line. With $\kappa_c \approx 2.27$ from numerical simulations[17], the extrapolation of our perturbative equations to $\alpha = 1$ would imply $\sigma \approx 0.2$, which is grossly too small. It indicates that while qualitatively correct, and valid in the perturbative region of parameters, the RG equations (5,6) are inadequate for quantitative estimations.

To obtain quantitative relations between the model parameters $\{J_{ab}, J_c, \Delta\}$ and experimental quantities, such as the in-plane and inter-plane correlation lengths ξ_{ab} and ξ_c , we use an alternative approach. Intuitively, we implement the cross-over from quasi 2D to isotropic 3D scaling in two-steps. If the ground state is disordered (with some correlation length ξ) then an exact RG transformation should result with a model for which the correlation length $\xi(l) = \xi/l$. Similarly, any *bare anisotropic* 3D model with finite $\xi_{ab} > \xi_c \geq 1$ is mapped onto an *effective isotropic* 3D model with $\xi_{ab} = \xi_c$ when the coarse-grained block size $l_{ab} \times l_{ab} \times l_c$ is chosen with $l_{ab} = \xi_{ab}/\xi_c$ and $l_c = 1$. Our strategy is to map the

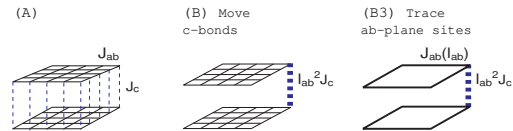


FIG. 3: Block transformation procedure

anisotropic RFIM onto a "solvable" isotropic 3D RFIM for which known properties enable us to derive estimates for $\xi_{ab}(J_{ab}, J_c, \Delta)$ and $\xi_c(J_{ab}, J_c, \Delta)$. In the absence of known exact RG equations for the RFIM, we resort to a Migdal-Kadanoff type RG procedure combined with our self-consistent scaling Ansatz (4). We adopt conventional approximations, ignoring the generation of longer range interactions [10], and using "majority rule" [15] for the value of the block spin variable. Hence, we follow only the transformation of effective nearest neighbor block interactions $J_{ab}(l)$, $J_c(l)$ and effective disorder $\Delta(l)$.

In the performance of a Migdal-Kadanoff transformation to blocks of size $l_{ab} \times l_{ab} \times 1$ (see Fig. 3), we first move the J_c bonds and thus create an effective block interaction $J_c(l_{ab}) = J_c l_{ab}^2$. Now that the c-axis coupling is removed, the planar $l_{ab} \times l_{ab}$ sections can be integrated out in a 2D fashion using our scaling Ansatz (4). The resulting RG equations are

$$J_c(l_{ab}) = J_c l_{ab}^2 \quad (7)$$

$$\kappa^{-2}(l_{ab}) = \kappa^{-2}\left[1 - \sigma\kappa^2 \ln(l_{ab})\right] \quad (8)$$

where $\kappa(l_{ab}) = \Delta(l_{ab})/J_{ab}(l_{ab})$. Our approximation procedure is equivalent to the assumption that fluctuations on length scale $l_{ab} < \xi_{ab}/\xi_c$ in ab -planes are uncorrelated in the c-axis direction. Since initially $J_c \ll \Delta$, it is initially indeed valid to integrate out over certain size of planar $l_{ab} \times l_{ab}$ sections, but the above assumption breaks down in the final stages of integration to the full block size $l_{ab} = \xi_{ab}/\xi_c$. This is the main source of error in our numerical estimates below. In addition, we need an explicit expression for $\Delta(l_{ab})$. The known perturbative expression for the surface tension per unit length on the scale l in 2D RFIM [10] $\Sigma(l) = J [1 - \sigma\kappa^2 \ln(l)]$ indicates that logarithmic corrections to $\kappa(l)$ come from the effective weakening of the inter-block interaction $J(l)$ due to the roughening of the "physical" domain boundaries. We are thus lead to maintain the Imry-Ma approximation for the scaling of disorder Δ under 2D block transformation to arrive at the final form of our approximate scaling equations for block $l_{ab} \times l_{ab} \times 1$;

$$J_c(l_{ab}) = J_c l_{ab}^2 \quad (9)$$

$$J_{ab}(l_{ab}) = J_{ab} l_{ab} \sqrt{1 - \sigma\kappa^2 \ln(l_{ab})} \quad (10)$$

$$\Delta(l_{ab}) = \Delta l_{ab}. \quad (11)$$

With the choice $l_{ab} = \xi_{ab}/\xi_c$, the correlation lengths in the transformed model are isotropic $\xi_{ab}(l_{ab} = \xi_{ab}/\xi_c) =$

ξ_c . Since the disorder correlations remain isotropic, it must be that the transformed interactions are also isotropic. Therefore, we impose the self-consistent requirement $J_{ab} (l_{ab} = \xi_{ab}/\xi_c) = J_c (\xi_{ab}/\xi_c)$. Thus we obtain a mapping of the bare anisotropic RFIM (1) onto an isotropic 3D RFIM with effective interactions

$$J_{ab} (l_{ab} = \xi_{ab}/\xi_c) = J_c (\xi_{ab}/\xi_c) = \left(\frac{\xi_{ab}}{\xi_c} \right)^2 J_c \quad (12)$$

and $\Delta (\xi_{ab}/\xi_c) = \left(\frac{\xi_{ab}}{\xi_c} \right) \Delta$. Using (10,11,12) and the correlation length of the 3D RFIM $\xi_{3D} = \Lambda (\kappa_c^{-2} - \kappa^{-2})^{-\nu} = \xi_c$, we obtain

$$\left(\frac{J_{ab}}{\Delta} \right)^2 = \kappa_c^{-2} - \left(\frac{\Lambda}{\xi_c} \right)^{1/\nu} + \sigma \ln (\xi_{ab}) \quad (13)$$

$$\left(\frac{J_c}{\Delta} \right)^2 = \left(\frac{\xi_c}{\xi_{ab}} \right)^2 \left[\kappa_c^{-2} - \left(\frac{\Lambda}{\xi_c} \right)^{1/\nu} \right]. \quad (14)$$

Substituting $\xi_c = 1$, we obtain an estimate of the crossover line $\xi_c \gtrless 1$ in the phase diagram; $\left(\frac{J_c}{J_{ab}} \right) = \sqrt{\kappa_c^{-2} - \Lambda^{1/\nu}} \left(\frac{J_{ab}}{\Delta} \right)^{-1} \exp \left\{ -\frac{1}{\sigma} \left[\left(\frac{J_{ab}}{\Delta} \right)^2 + \Lambda^{1/\nu} - \kappa_c^{-2} \right] \right\}$. With $\kappa_c \approx 2.27$, $\Lambda \approx 0.1$ and $\nu \approx 1.37$ (from numerical simulations[17]), equations (13,14) enable us to retrodict the effective model parameters. For $\text{La}_{0.5}\text{Sr}_{1.5}\text{CoO}_4$ (Table-1 V) we find $\frac{\Delta}{J} \approx 0.76$, and $\frac{J_{ab}}{J_c} > 106$, indeed satisfying the relations $J_c \ll \Delta < J_{ab}$ under which our approximations are valid. For $\text{La}_{0.5}\text{Sr}_{1.5}\text{MnO}_4$ (Table-1 IV) $\frac{\Delta}{J_{ab}} \approx 0.6$ and $\frac{J_{ab}}{J_c} \approx 74$. The anisotropy of the bare coupling parameters is remarkably high! Yet, we think it is quite realistic for the layered systems. Because neighbor ab -planes are shifted so that MO_6 octahedra in one plane fit in-between those in the other (see Fig. 1(f)), and the inter-plane spacing is rather large, breathing-type distortions of the octahedra accompanying the CO are weakly coupled between the planes. On the other hand, octahedra within each plane form a corner-sharing network, so the coupling of in-plane distortions is strong. In the pseudocubic perovskite structure, the MO_6 octahedra share apical oxygens along the c -axis as well (see Fig. 1(e)), and crystal fields are more isotropic. Note that, for a system to have a LRO groundstate, interactions need not be isotropic. For weak disorder, the phase diagram instructs us that in fact only very strongly anisotropic systems will be disordered (as exemplified by our above estimates of J_{ab}/J_c in the layered compounds).

In conclusion, on general grounds we argued that the charge order observed in half-doped manganites and their isostructural relatives is described by an *anisotropic* ($J_c \neq J_{ab}$) 3D random field Ising model (1). We introduced the schematic phase diagram of this model (Fig.2),

and supported its intuitive structure by perturbative RG equations (5,6). We estimated the effective model parameters values for given measured correlation lengths, using a phenomenological scaling equation (4) and a block transformation scheme.

Long-range charge order is observed in the pseudocubic compounds at low temperatures. In contrast, a disordered ground state with anisotropic correlations is found in the layered materials. This disparity is naturally explained by our model as systems residing in the different regions of the phase diagram. We note that the disordered 3D RFIM has well known features which may be verified experimentally. Furthermore, our analysis may be applied to thin films, where even for the pseudocubic materials correlations in one direction are limited by the film thickness. The latter together with the model parameters will then determine the CO correlation length within the film. Finally, we note that charge disorder in the form of dislocations, as in Fig. 1(d), has inevitable effects on the superimposed orbital and spin orders which are thus far not elaborated.

We thank J.P. Hill, S. A. Kivelson and A. Tsvelik for fruitful discussions, and acknowledge the financial support of DOE#DE-AC02-98CH10886 (O.Z. and I.Z.) and DOE#DE-FG03-00ER45798 (O.Z.).

- [1] A. Millis, B. I. Shraiman, P. B. Littlewood, Phys. Rev. Lett. **74**, 5144 (1995).
- [2] E. Dagotto, T. Hotta, A. Moreo, Physics Reports **344** (2001).
- [3] E.L. Nagaev, Physics Reports **346**, 387 (2001).
- [4] B. J. Sternlieb *et al.*, Phys. Rev. Lett. **83**, 4872 (1996).
- [5] I. A. Zaliznyak *et al.*, Phys. Rev. Lett. **85**, 4353 (2000); I. A. Zaliznyak *et al.*, Phys. Rev. B **64**, 195117 (2001).
- [6] Among pseudocubic manganites such CO occurs in some Sr-doped and most of the Ca-doped systems, but not in $\text{La}_{0.5}\text{Sr}_{0.5}\text{MnO}_3$ and $\text{Pr}_{0.5}\text{Sr}_{0.5}\text{MnO}_3$.
- [7] G. A. Gehring and K. A. Gehring, Rep. Prog. Phys. **38**, 1 (1975).
- [8] Y. Imry and S. K. Ma, Phys. Rev. Lett. **35**, 1399 (1975).
- [9] A. Aharony, Y. Imry, S. K. Ma, Phys. Rev. Lett. **37**, 1364 (1976); G. Grinstein, Phys. Rev. Lett. **37**, 944 (1976).
- [10] For a review see T. Nattermann and J. Villain, Phase Trans. **11**, 5 (1987).
- [11] P. G. Radaelli, D. E. Cox, M. Marezio, S.-W. Cheong, Phys. Rev. B **55**, 3015 (1997).
- [12] M. v. Zimmermann *et al.*, Phys. Rev. Lett. **76**, 2169 (1999).
- [13] K. Nakamura *et al.*, Phys. Rev. B **60**, 2425 (1999).
- [14] Y. Wakabayashi *et al.*, J. Phys. Soc. Jpn. **70**, 1194 (2001).
- [15] Leo P. Kadanoff, Ann. of Phys., **100**, 359 (1976).
- [16] John Cardy, “*Scaling and Renormalization in Statistical Physics*”, Cambridge U. Press (1996).
- [17] A.A. Middleton and D.S. Fisher, cond-mat/0107489.